Nageswara Rao, B. D., & Cohn, M. (1977) *Proc. Natl. Acad. Sci. U.S.A. 74*, 5355-5357.
Noda, L. (1958) *J. Biol. Chem. 232*, 237-250.
Pace, C. N. (1986) *Methods Enzymol. 131*, 266-280.
Ray, B. D., Rösch, P., & Nageswara Rao, B. D. (1988) *Biochemistry 27*, 8669-8676.
Reinstein, J., Vetter, I. R., Schlichting, I., Rösch, P., Wittinghofer, A., & Goody, R. (1990) *Biochemistry 29*, 7440-7450.
Rhoads, D. G., & Lowenstein, J. M. (1986) *J. Biol. Chem. 243*, 3963-3972.
Sanders, C. R., II, Tian, G., & Tsai, M.-D. (1989) *Biochemistry 28*, 9028-9043.
Sanders, C. R., II, & Tsai, M.-D. (1989) *Methods Enzymol. 177*, 317-333.
Schlichting, I., Almo, S. C., Rapp, G., Wilson, K., Petratos, K., Lentfer, A., Wittinghofer, A., Kabsch, W., Pai, E. F., Petsko, G. A., & Goody, R. S. (1990) *Nature 345*, 309-315.
Schulz, G. E. (1987) *Cold Spring Harbor Symp. Quant. Biol. 52*, 429-439.
Smith, G. M., & Mildvan, A. S. (1982) *Biochemistry 21*, 6119-6123.
Tanizawa, Y., Kishi, F., Kaneko, T., & Nakazawa, A. (1987) *J. Biochem. (Tokyo) 101*, 1289-1296.
Taylor, J. W., Schmidt, W., Cosstick, R., Okruszek, A., & Eckstein, F. (1985a) *Nucleic Acid Res. 13*, 8749-8764.
Taylor, J. W., Ott, J., & Ecstein, F. (1985b) *Nucleic Acid Res. 13*, 8764-8785.
Tian, G., Sanders, C. R., II, Kishi, F., Nakazawa, A., & Tsai, M.-D. (1988) *Biochemistry 27*, 5544-5552.
Tian, G., Yan, H., Jiang, R.-T., Kishi, F., Nakazawa, A., & Tsai, M.-D. (1990) *Biochemistry 29*, 4296-4304.
Tsai, M.-D., Drakenberg, T., Thulin, E., & Forsén, S. (1987) *Biochemistry 26*, 3635-3643.
Yan, H., Shi, Z., & Tsai, M.-D. (1990a) *Biochemistry 29*, 6385-6392.
Yan, H., Dahnke, T., Zhou, B., Nakazawa, A., & Tsai, M.-D. (1990b) *Biochemistry 29*, 10956-10964.
Zimmerman, S. C., & Cramer, K. D. (1988) *J. Am. Chem. Soc. 110*, 5906-5908.

Laser Flash Photolysis Studies of the Kinetics of Electron-Transfer Reactions of *Saccharomyces* Flavocytochrome b_2: Evidence for Conformational Gating of Intramolecular Electron Transfer Induced by Pyruvate Binding†

Mark C. Walker‡ and Gordon Tollin*
Department of Biochemistry, University of Arizona, Tucson, Arizona 85721
Received August 23, 1990; Revised Manuscript Received March 5, 1991

ABSTRACT: The kinetics of reduction of the flavocytochrome from *Saccharomyces cerevisiae* by exogenous deazaflavin semiquinones have been investigated by using laser flash photolysis. Direct reduction by deazaflavin semiquinone of both the b_2 heme and the FMN cofactor occurred via second-order kinetics with similar rate constants (9×10^8 M^{-1} s^{-1}). A slower, monoexponential, phase of FMN reoxidation was also observed, concurrent with a slow phase of heme reduction. The latter accounted for approximately 20–25% of the total heme absorbance change. Both of these slow phases were protein concentration dependent, yielding indentical second-order rate constants (1.1×10^7 M^{-1} s^{-1}), and were interpreted as resulting from intermolecular electron transfer from the FMN semiquinone on one protein molecule to an oxidized heme on a second molecule. Consistent with this conclusion, no slow phase of heme reduction was observed with deflavo-flavocytochrome b_2. Upon the addition of pyruvate (but not D-lactate or oxalate), the second-order rate constant for heme reduction was unaffected, but direct reduction of the FMN cofactor was no longer observed. Reduction of the heme cofactor was followed by a slower partial reoxidation, which occurred concomitantly with a monoexponential phase of FMN reduction. Both processes were protein concentration independent and were interpreted as the result of intramolecular electron transfer from reduced b_2 heme to oxidized FMN. Potentiometric titrations of the flavocytochrome in the absence and presence of pyruvate demonstrated that the thermodynamic driving force for electron transfer from FMN to heme is much greater in the absence of pyruvate. Despite this, intramolecular electron transfer was only observed in the presence of pyruvate. This result is interpreted in terms of a conformational change induced by pyruvate binding which permits electron transfer between the cofactors. The rate constant for intramolecular electron transfer in the presence of pyruvate was dependent on ionic strength, suggesting the occurrence of electrostatic effects which influence this process.

Yeast flavocytochrome b_2 (L-lactate dehydrogenase, EC 1.1.2.3) is a bifunctional enzyme (Jacq & Lederer, 1974) that catalyzes the two-electron oxidation of L-lactate to pyruvate, and subsequent one-electron transfers to two cytochrome *c* molecules (Labeyrie et al., 1978; Capeillere-Blandin et al., 1980; Labeyrie, 1982). The protein exists in solution as a tetrameric assembly of monomers, each with a molecular weight of 57 500. The crystal structure for the enzyme from *Saccharomyces cerevisiae* has been determined at 2.4-Å resolution (Xia et al., 1987; Mathews & Xia, 1987; Xia & Mathews, 1990) and demonstrates that the monomer is folded into two functionally distinct domains. The flavodehydrogenase domain contains the FMN[1] cofactor, substrate

† This work was supported in part by Grant DK15057 from the National Institutes of Health (to G.T.).
* To whom correspondence should be addressed.
‡ Present address: Monsanto Agricultural Co., 800 N. Lindbergh Blvd., St Louis, MO 63167.

0006-2960/91/0430-5546$02.50/0

binding pocket, and amino acid residues pertinent to the oxidation of lactate (Reid et al., 1988). The cytochrome domain contains the b_2 heme cofactor and is the site at which the protein is reoxidized by cytochrome *c*. From the crystal structure, the geometries of the heme and flavin cofactors within the protein appear to be well suited for efficient electron transfer. They are separated by a distance of 9.7 Å from heme edge to flavin and are approximately coplanar. The propionate group of the heme A ring extends toward the flavin ring and forms hydrogen-bonding interactions with Tyr-143 of the flavodehydrogenase domain and, via a bridging water molecule, with the N5 and O4 of the flavin ring. The aromatic ring of Tyr-143 is nearly perpendicular to the flavin and heme rings.

The kinetics of substrate binding and the two-electron reduction of FMN have been examined previously and are well characterized (Lederer, 1974; Capeillere-Blandin et al., 1975, 1986; Pompon et al., 1980). Likewise, the binding of cytochrome *c* and subsequent one-electron transfer from b_2 heme have also been the subject of much interest (Capeillere-Blandin et al., 1980; Capeillere-Blandin, 1982; Matsushima et al., 1986; Capeillere-Blandin & Albani, 1987). However, intramolecular electron transfer between the FMN and b_2 cofactors, an obligatory step prior to reoxidation by cytochrome *c*, has proven to be more difficult to examine. This difficulty is partly due to the fact that hydrogen abstraction from substrate and reduction of FMN are catalytically rate limiting (Lederer, 1974). Consequently, heme reduction is observed to occur concurrently with flavin reduction following the rapid mixing of protein with substrate under anaerobic conditions (Ogura & Nakamura, 1966; Suzuki & Ogura, 1970; Capeillere-Blandin, 1975; Capeillere-Blandin et al., 1975, 1986; Pompon et al., 1980). A small lag in the formation of FMN semiquinone has provided a basis for computer simulations of transient absorbance changes obtained during stopped-flow experiments. These have generated estimates for the rate constants for intramolecular electron transfer between flavin and heme cofactors (Capeillere-Blandin, 1975; Pompon, 1980; Capeillere-Blandin et al., 1986). It should be noted, however, that the data obtained from stopped-flow experiments mainly reflect electron transfer from fully reduced FMN to oxidized heme.

Intramolecular electron transfer has also been examined by using the pulse radiolysis technique (Capeillere-Blandin et al., 1984) to rapidly introduce reducing equivalents, and by equilibrium perturbation of partially reduced flavocytochrome by a temperature jump (Tegoni et al., 1984). Spectral changes observed during pulse radiolysis experiments were consistent with the direct reduction of heme, with no indication of FMN reduction. Spectral changes observed during the temperature jump studies suggested that intramolecular reduction of heme by FMN semiquinone occurred; however, the kinetics were complex and difficult to interpret.

We have examined the kinetics of reduction of the flavocytochrome b_2 from *Saccharomyces cerevisiae* by deazaflavin semiquinones, generated in situ by laser flash photolysis. Unlike the pulse radiolysis experiments, direct reduction of both the FMN and b_2 cofactors was obtained. As will be demonstrated below, intramolecular electron transfer was observed *only* in the presence of pyruvate (the product arising from catalytic oxidation of lactate) despite apparently favorable conditions of cofactor orientation and thermodynamic driving force. Preliminary experiments indicate that the protein from *Hansenula anomala* behaves similarly. The results are interpreted in terms of an electron-transfer mechanism which is controlled by changes in protein conformation mediated by the binding of pyruvate.

Materials and Methods

Flavocytochrome b_2 from *Saccharomyces cerevisiae* was purified as described for the "intact" noncrystalline form by Labeyrie et al. (1978). Ratios of UV absorbance to that of the Soret band (423 nm) for the reduced b_2 heme were consistent with literature values. The molar activity of protein preparations (expressed per monomeric heme) ranged from 450 to 530 s^{-1}, as determined by the reduction of $K_3Fe(CN)_6$ during enzymatic oxidation of L-lactate at 30 °C (Labeyrie et al., 1978). The purified protein was stored as an ammonium sulfate precipitate at 4 °C in the presence of DL-lactate. Protein aliquots were recovered from storage by diluting the suspension 3-fold with 0.1 M phosphate buffer, pH 7.0, followed by chromatography over Sephadex G-25 to exchange salts and reoxidize the protein. Working stock solutions were prepared by concentrating the eluate to approximately 1 mM heme using a Centricon 10 microconcentrator (Amicon Corp., Danvers, MA). During flash photolysis experiments, protein concentrations were determined from absorbancies at either 413 nm (oxidized form) or 423 nm (reduced form) using extinction coefficients of 129.5 and 183 mM^{-1} cm^{-1}, respectively (Labeyrie et al., 1978). During potentiometric titrations, protein concentrations were determined from absorbancies at either 530 nm (oxidized form) or 557 nm (reduced form) using extinction coefficients of 11.3 and 30.9 mM^{-1} cm^{-1}, respectively (Labeyrie et al., 1978). *Saccharomyces* deflavo-flavocytochrome b_2 was prepared from the holoprotein as described by Baudras (1962). Deazariboflavin (dRf) was prepared according to the method of Smit et al. (1986). 5-Deazalumiflavin-3′-propanesulfonate (dLfS) was a generous gift from Dr. T. C. Bruice. Potassium phosphate buffer, pH 7.0, was used in concentrations as specified in the figure legends. Semicarbazide (SC) or ethylenediaminetetraacetic acid (EDTA) were included in the buffers to act as sacrificial electron donors for triplet-state flavins. Sodium pyruvate was obtained from Sigma Chemical Co. (St. Louis, MO) and was recrystallized from water/ethanol as required.

Steady-state kinetic assays were performed at 30 °C in a 1-mL assay volume of 5.7 mM phosphate buffer, pH 7.0, containing 1 mM EDTA and 1 mM $K_3Fe(CN)_6$. Ionic strength was adjusted by the inclusion of NaCl to this buffer. Reaction time courses were monitored by the absorbance changes at 420 nm resulting from the reduction of ferricyanide, using a Cary 15 spectrophotometer. Unless otherwise noted, steady-state kinetic rate constants were expressed in terms of moles of electron equivalents transferred per monomeric heme.

All laser photolysis experiments were performed anaerobically at ambient temperature (23–25 °C) in cuvettes containing 1 mL of a buffer solution containing deazaflavin plus SC, which were deaerated by alternating cycles of vacuum and argon flush. Microliter volumes of a concentrated solution of protein were added via a Hamilton syringe to the sealed cuvette after deaeration. Laser photoexcitation was carried out with a nitrogen laser pumped dye solution (BBQ 2A386 dye from PRA, 396-nm maximum wavelength). A detailed

[1] Abbreviations: FMN and $FMNH_2$, oxidized and two-electron-reduced flavin mononucleotide, respectively; F_{ox}, F_{sq}, and F_{red}, oxidized, one-electron-reduced, and two-electron-reduced FMN, respectively; H_{ox} and H_{red}, oxidized and reduced b_2 heme, respectively; dLfS and dLfSH•, oxidized and one-electron-reduced 5-deazalumiflavin-3′-propanesulfonate, respectively; dRf and dRfH•, oxidized and one-electron-reduced 5-deazariboflavin, respectively; EDTA, ethylenediaminetetraacetic acid; SC, semicarbazide hydrochloride; k_{obs}, observed rate constant; k_f and k_r, forward and reverse microscopic rate constants, respectively, E_1, first one-electron reduction potential of the FMN cofactor ($FMN_{ox} + e^- \rightarrow FMN_{sq}$); E_2, second one-electron reduction potential of the FMN cofactor ($FMN_{sq} + e^- \rightarrow FMN_{red}$).

description of the laser flash apparatus and the method of data collection has been published elsewhere (Bhattacharyya et al., 1983; Przysiecki et al., 1985). The concentrations of deazaflavin semiquinone produced by the laser flash were estimated from absorbance changes observed at 510 nm immediately (<20 μs) following the laser flash using a Δ extinction coefficient of 3.5 mM^{-1} cm^{-1} (Visser & Fendler, 1982; Heelis et al., 1989).

Laser flash photolysis generated deazaflavin semiquinone which, in the absence of protein, underwent disproportionation. In the presence of protein, electron transfer from the semiquinone occurred to produce reduced protein. Consequently, semiquinone disporportionation was always in competition with protein reduction. The contribution of the disproportionation reaction to the observed transient decay kinetics is determined by the magnitude of the second-order rate constant for protein reduction and the concentrations of the reacting species (i.e., protein vs semiquinone). The second-order rate constants for protein reduction obtained in the present experiments were generally on the order of 10^9 M^{-1} s^{-1}. Therefore, complications arising as a result of flavin disproportionation were insignificant. Consistent with this, the absorbance changes corresponding to direct reduction of protein by exogenous deazaflavin semiquinones were well fit by a single exponential with a corresponding rate constant which was protein concentration dependent. All kinetic experiments were performed under pseudo-first-order conditions in which the concentration of protein acceptor (>2 μM) was in excess over the amount of semiquinone produced per flash (localized concentration <0.6 μM). This assures that only a single electron enters each protein molecule. Transient absorbance changes were analyzed by using a computer-fitting procedure (SIFIT; obtained from OLIS Co., Jefferson, GA). Unless quantitation was required (e.g., for absorbance change measurements), the number of flashes averaged per kinetic trace varied.

Potentiometric titrations were performed following the methodology of Wilson (1978) and of Stankovich (1980), with the modification that methyl viologen radical ($MV^{\bullet+}$) was generated photochemically using dRf in the presence of EDTA. This was necessary inasmuch as attempts to reduce or oxidize the protein using electrochemically generated titrants resulted in excessive protein precipitation. The presence of methyl viologen (0.1 mM) avoided the formation of the unreactive $dRfH_2$ species as a result of $dRfH^{\bullet}$ disproportionation. Fe-EDTA ($E_{m,7}$ = +117 mV), methylene blue (+11 mV), pyocyanine (−34 mV), and 2-hydroxy-1,4-naphthoquinone (−137 mV) were included as mediators (Fultz & Durst, 1982), each at a concentration of 3 μM, in order to facilitate communication between the protein and the electrodes. Electrochemical potentials were measured vs a Ag/AgCl reference electrode which had been stored anaerobically. The standard potential of the reference electrode was calibrated relative to a saturated quinhydrone solution (+575.5 mV at 25 °C; O'Reilly, 1973; Clark, 1960) following each experiment. All potentials are reported relative to the standard hydrogen electrode (SHE).

Potentiometric phototitrations of 20–30 μM flavocytochrome b_2 were performed in the absence and presence of 5 mM pyruvate under conditions similar to those used during the flash photolysis experiments. In order to minimize photoinactivation of the oxidized protein while in the presence of pyruvate (Blazy, 1982; Tegoni et al., 1986), a filter was employed to remove wavelengths above 420 nm from the light source used for photoreduction. Spectra were recorded and stored by using an On-Line Instruments update of a Cary-15 spectrophotometer (OLIS Co., Jefferson, GA) interfaced with an AT microcomputer. In order to account for small changes in base line which occurred during the course of the titration, spectra were normalized at 545 nm (Tegoni et al., 1986), which corresponds to an experimentally observed isosbestic point for heme reduction. Heme reduction levels were determined from absorbance measurements at 557 nm. Flavin reduction levels were determined from the absorbance changes at 450 nm, following removal of the absorbance contribution due to the reduction of b_2 heme. The absorbance contribution at 450 nm resulting from heme reduction accounted for 48% of the total bleach observed upon complete reduction of the holo form (Capeillere-Blandin et al., 1975; Tegoni et al., 1986). Spectral changes associated with the reduction of mediator dyes represented less than 2% of the total absorbance change observed at 557 or 450 nm, and were therefore ignored.

RESULTS

Difference Spectra Obtained upon Flavocytochrome b_2 Reduction. Time-resolved difference spectra constructed from absorbance changes following the laser flash are presented in Figure 1. In the absence of protein, a broad band of increased absorbance centered at 510 nm due to the deazaflavin semiquinone was observed immediately (<20 μs) following the laser flash (Figure 1a). One-electron reduction of dLfS has a large negative midpoint potential ($E_{m,7}$ = −650 mV; Blankenhorn, 1976), and the semiquinone species is, therefore, a suitable electron donor for reduction of flavocytochrome. In the presence of protein, the time-resolved difference spectrum obtained 50 ms after the laser flash (open circles in Figure 1b) is similar to that for the substrate reduced-minus-oxidized steady-state difference spectrum of the flavocytochrome (solid line in Figure 1c). This observation demonstrates that reducing equivalents generated during the laser flash resulted in protein reduction. Note that the wavelength corresponding to the maximum absorbance of the deazaflavin semiquinone (510 nm) also corresponds to an isosbestic point observed during the reduction of flavocytochrome. Consequently, at this wavelength, the reoxidation of the deazaflavin semiquinone can be monitored independently of protein reduction. On the basis of the Δ extinction coefficients for deazaflavin semiquinone at 510 nm (3.5 mM^{-1} cm^{-1}; Visser & Fendler, 1982; Heelis et al., 1989) and flavocytochrome at 557 nm (21.5 mM^{-1} cm^{-1}; Labeyrie et al., 1978), the absorbance contribution due to the deazaflavin semiquinone is expected to be less than 4% and 10% of the total absorbance changes observed at 557 at 450 nm, respectively, during the reduction of protein. Furthermore, the deazaflavin semiquinone was observed to be completely reoxidized within several milliseconds in the presence of protein (see below). Consequently, no spectral contribution due to this species is expected at any wavelength following the fast phase of protein reduction.

The absorbance changes observed at 557 nm following reduction of flavocytochrome b_2 contain only contributions from reduced heme, while those observed at 450 nm contain contributions from both reduced heme and FMN (Capeillere-Blandin et al., 1975; Tegoni et al., 1986). Comparison of the ratios of $\Delta A_{557}/\Delta A_{450}$ obtained with the holo- and deflavoproteins can thus provide information on the relative accessibility of reducing equivalents to the FMN and heme cofactors. A $\Delta A_{557}/\Delta A_{450}$ ratio of 1.75 was obtained from the time-resolved flash photolysis difference spectrum of the holoprotein (cf. open circles in Figure 1b). Values of 1.33 and 2.60 were obtained from a substrate reduced-minus-oxidized steady-state difference spectrum of the holoprotein (solid line in Figure 1c) and a photoreduced-minus-oxidized steady-state difference spectrum of the deflavo-flavocytochrome b_2 (dashed

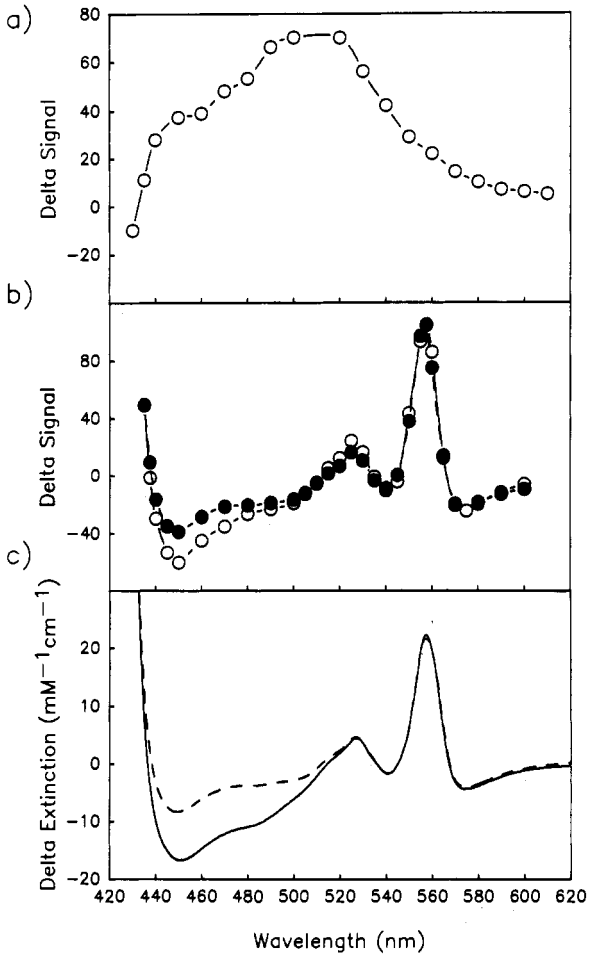

FIGURE 1: Transient reduced-minus-oxidized difference spectra obtained from the flash-induced absorbance changes observed with the following: (a) 160 μM dLfS in 5.7 mM phosphate buffer, pH 7.0, containing 0.5 mM SC, approximately 20 μs following the laser pulse; (b) 13.6 μM flavocytochrome (open circles) or 12.5 μM deflavoflavocytochrome (closed circles) plus 114 μM dLfS in 50 mM phosphate, pH 7.0, containing 0.5 mM SC, approximately 50 ms following the laser pulse. The absorbance scales are expressed in arbitrary units. (c) Substrate reduced-minus-oxidized steady-state difference spectrum of 9.1 μM flavocytochrome (solid line) in 0.1 M phosphate, pH 7.0, containing 1 mM EDTA, and photoreduced-minus-oxidized steady-state difference spectrum of 13.7 μM deflavo-flavocytochrome (dashed line) in 0.1 M phosphate, pH 7.0, containing 1 mM EDTA and 20 μM dLfS.

line in Figure 1c), respectively. These results indicate that approximately 30–40% of the reducing equivalents generated during the flash entered the protein at the FMN cofactor site, with the remainder entering at the heme site of a separate protein molecule. For comparison, a $\Delta A_{557}/\Delta_{A450}$ ratio of 2.69 was obtained from the time-resolved flash photolysis difference spectrum of the deflavoprotein (solid circles in Figure 1b), consistent with that obtained from steady-state photoreduction (2.60; dashed line in Figure 1c).

Kinetics of Flavocytochrome b_2 Reduction in the Absence of Ligands. In the presence of protein, a biphasic increase in absorbance was observed at 557 nm immediately following the laser flash (Figure 2a,b), corresponding to heme reduction. The observed rate constants (k_{obs}) for both phases were dependent on protein concentration, yielding second-order rate constants of 9.2×10^8 and 1.1×10^7 M^{-1} s^{-1} (open circles in insets to figure 2a,b) for the fast and slow phases of heme reduction, respectively. Control experiments using deazariboflavin semiquinone (dRfH$^\bullet$) as the reductant also gave biphasic heme reduction, with comparable second-order rate constants for the fast and slow phases (7.1×10^8 and $1.5 \times$

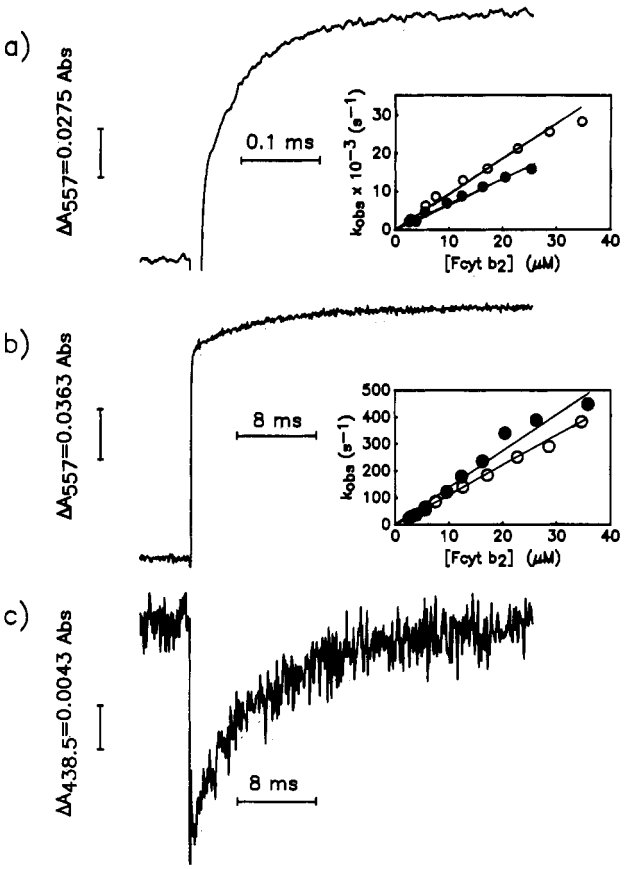

FIGURE 2: (a, b) Transient absorbance changes at 557 nm in the presence of 17 μM flavocytochrome. The buffer conditions were 0.1 M phosphate, pH 7.0, containing 140 μM dLfS and 1 mM SC. Insets represent second-order plots of k_{obs} vs concentration during the reduction of protein by dLfS (open circles) and dRf (closed circles) semiquinones. (c) Transient absorbance changes at 438.5 nm in the presence of flavocytochrome. Conditions were identical with those in (a) and (b). All plots represent the sum of 10 flashes.

10^7 M^{-1} s^{-1}, respectively; cf. closed circles in insets to Figure 2a,b). The slow phase of heme reduction accounted for approximately 20–25% of the total signal observed at 557 nm (Figure 2b).

Transient absorbance changes at 510 nm displayed an initial absorbance increase which decayed monoexponentially to the preflash base line (data not shown). This wavelength is near an isosbestic point for protein reduction (cf. Figure 1b). Therefore, this absorbance decay represents the reoxidation of the deazaflavin semiquinone generated during the laser flash. The observed pseudo-first-order rate constants obtained from these absorbance changes were comparable to those for the fast phase of heme reduction, indicating that this fast phase results from the direct reduction of protein by electron transfer from dLfS semiquinone.

The kinetics of reduction of flavocytochrome b_2 were also monitored at 438.5 nm. This wavelength is near an isosbestic point for the reduction of the b_2 heme (Baudras, 1965; Labeyrie et al., 1966). Therefore, absorbance changes at this wavelength are dominated by the reduction of the FMN cofactor. At this wavelength, the Δ extinction coefficient for the deazaflavin semiquinone is approximately 0.7 mM^{-1} cm^{-1} (from Figure 1a), while that for the reduction of the FMN cofactor is −7.9 mM^{-1} cm^{-1} (Labeyrie et al., 1978). Transient absorbance changes at 438.5 nm are illustrated in Figure 2c. An initial fast phase of absorbance decrease occurred on a time scale similar to that used to monitor the fast phase of heme reduction (data not shown). This absorbance bleach was also concentration dependent. The signal-to-noise ratios of these

traces would not allow an accurate determination of a second-order rate constant for FMN reduction. However, the data were consistent with a value similar to that for the fast phase of heme reduction. The initial bleach of absorbance is interpreted as resulting from the direct reduction of the FMN cofactor by deazaflavin semiquinone.

The rapid loss of absorbance at 438.5 nm was followed by a slow reappearance of absorbance (cf. Figure 2c) which occurred on the same time scale as that observed for the slow phase of heme reduction (compare with Figure 2b). This was interpreted as being due to the reoxidation of the FMN semiquinone by electron transfer to the oxidized b_2 heme. The slow absorbance changes representing FMN semiquinone reoxidation were also protein concentration dependent (data not shown), giving the same second-order rate constant as obtained for the slow phase of heme reduction. This indicates that the electron transfer was bimolecular, occurring between one-electron reduced FMN and oxidized heme centers of distinct tetrameric assemblies of the flavocytochrome complex.

No evidence for a protein *concentration independent* exchange of electrons between the FMN and heme cofactors was observed in the present flash experiments at protein concentrations as high as 30 μM. We estimate that the intramolecular transfer would have been readily detected from transient absorbance changes at 557 nm if such a process had a rate constant of 10^4 s^{-1} or less.

The kinetics of reduction of the deflavo-flavocytochrome were examined in order to provide additional support for the assignment of the slower absorbance changes to intermolecular electron transfer between FMN and b_2 cofactors. With the deflavoenzyme, a second-order rate constant of 1.0×10^9 M^{-1} s^{-1} was obtained for the direct reduction of heme by dLfSH$^\bullet$ (data not shown). This value is the same as that obtained for the fast phase of heme reduction using the holoprotein. No slow phase of heme reduction was observed over a time course of several hundred milliseconds (not shown), which supports the conclusion that the slow phase represents electron transfer from FMN semiquinone to b_2 heme.

Kinetics of Flavocytochrome b_2 Reduction upon Pyruvate Addition. In the presence of 5 mM pyruvate, transient absorbance changes at 557 nm displayed an initial rapid increase in absorbance corresponding to heme reduction (Figure 3a), which was then followed by a slower absorbance decrease due to heme reoxidation (Figure 3b; compare with Figure 2b). The initial absorbance increase was protein concentration dependent, yielding a second-order rate constant of 8.7×10^8 M^{-1} s^{-1} (inset to Figure 3a). This value is within experimental error the same as that obtained for the fast phase of heme reduction in the absence of pyruvate. A slow loss of absorbance at 438.5 nm, corresponding to the reduction of FMN, was observed on a time scale comparable to that of heme reoxidation (Figure 3c). The absorbance decreases observed at 557 and 438.5 nm were both protein concentration *independent* (inset to Figure 3c; $k = 615$ s^{-1}), and thus can be interpreted as resulting from intramolecular electron transfer from reduced b_2 heme to oxidized FMN. Consistent with this interpretation, no slow phase of heme reoxidation was observed with the deflavo-flavocytochrome b_2 in the presence of 5 mM pyruvate (not shown). Due to the nature of the isobestic point at 438.3 nm and the large bandwidth of the optical system used for data collection, an accurate comparison of the extents of flavin reduction and heme reoxidation was not possible. No rapid absorbance bleach due to direct reduction of the FMN was observed during the transient absorbance changes at 438.5 nm (Figure 3c; compare with Figure 2c), indicating that the FMN

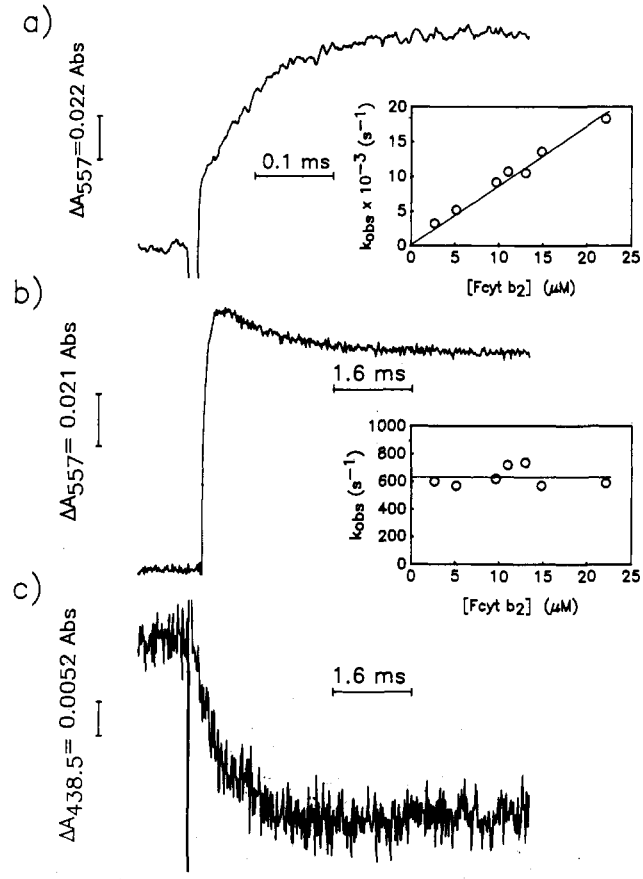

FIGURE 3: Transient absorbance changes at 557 nm obtained during the reduction of flavocytochrome in the presence of pyruvate using (a) 0.5-ms and (b) 8-ms time scales. Insets represent second-order plots of k_{obs} vs concentration during the reduction of protein by dLfS semiquinone. (c) Transient absorbance changes at 438.5 nm using a 8-ms time scale. Conditions were 11 μM flavocytochrome in 50 mM phosphate, pH 7.0, containing 140 μM dLfS, 1 mM SC, and 5 mM pyruvate.

cofactor is inaccessible to the exogenous reductant once pyruvate is bound at the active site.

The effect of pyruvate on the observed kinetic behavior was examined over the concentration range of 1–10 mM. At the lowest pyruvate concentration, a kinetic pattern was obtained which was intermediate between that observed in the absence and in the presence of 5 mM pyruvate. As the concentration of pyruvate was increased, the amplitude of the signal corresponding to heme reoxidation increased, whereas the signal corresponding to the slow phase of heme reduction decreased in amplitude. These changes were most apparent at approximately 3 mM pyruvate. Little or no additional change in the kinetic behavior of the enzyme was observed at pyruvate concentrations higher than 5 mM. Furthermore, this change in kinetic properties was specific for pyruvate, and was not observed in the presence of D-lactate or oxalate.

Similar results were observed with the flavocytochrome b_2 from *Hansenula anomala* when pyruvate was included in laser flash photolysis experiments. A complete description of the kinetics of reduction of this protein will be reported elsewhere.

The rate constant for intramolecular electron transfer between FMN and heme cofactors of *Saccharomyces* flavocytochrome b_2 displayed a dependence on ionic strength (Figure 4), decreasing from 1200 s^{-1} at $I = 10$ mM to 400 s^{-1} at $I = 500$ mM. In order to determine if this effect was a result of ionic strength dependent changes in the binding affinity for pyruvate, the inhibition of the steady-state oxidation of L-lactate in the presence of pyruvate was examined (Lederer,

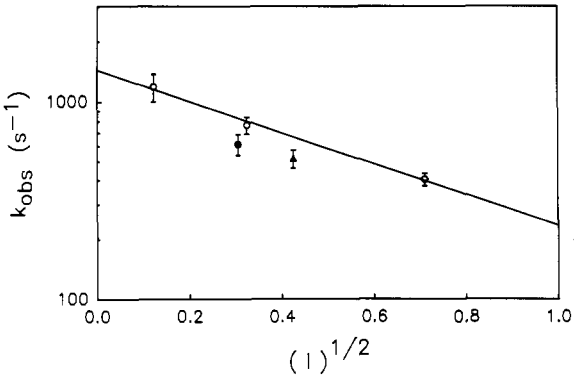

FIGURE 4: Ionic strength dependence of the rate constant for intramolecular electron transfer between heme and FMN cofactors, obtained in the presence of 5 mM pyruvate. Buffer conditions were as follows: (○) 5.7 mM phosphate, pH 7.0, containing 0.5 mM SC and increasing amounts of NaCl; (●) 50 mM phosphate, pH 7.0, containing 1 mM SC; (▲) 100 mM phosphate, pH 7.0, containing 1 mM SC.

1978). A K_i of 3.7 mM for competitive inhibition by pyruvate was obtained (not shown) at I = 100 mM, in agreement with reported values (Lederer, 1978). This constant was essentially unaffected by changes in ionic strength. Although a value for K_i cannot be equated with the dissociation constant (K_d) for pyruvate binding (Cleland, 1963; Tegoni et al., 1990), this result suggests that the decrease in the rate constant for intramolecular electron transfer observed as the ionic strength was increased may be a consequence of charge-pair interactions which influence protein conformation (see below).

The rate constant for intramolecular electron transfer also displayed a dependence on the buffer conditions. Values obtained in the presence of 50 or 100 mM phosphate buffer (cf. closed circles, Figure 4) were different from those obtained in the presence of 5.7 mM phosphate at comparable ionic strengths. Such differences can be attributed to a specific effect of phosphate ions. Similar effects due to phosphate have been observed on the rate constant for electron transfer between the ferredoxin and ferredoxin–$NADP^+$ reductase isolated from spinach (Walker, unpublished data). The binding of various divalent anions to *c*-type cytochromes, and the resulting alterations in midpoint potential, has also been noted previously (Gopal et al., 1988). Thus, it is not unreasonable to suggest that a divalent anion such as phosphate may interact with proteins differently than monovalent anions such as chloride (Ferguson-Miller et al., 1976; Malatesta et al., 1987).

The amplitude of the absorbance changes collected in the presence of pyruvate was observed to decrease with time; an approximately 50% reduction in signal was observed within 1 h following the addition of the pyruvate stock solution to the protein-containing cuvette. This decrease in signal amplitude was associated with a decrease in the yield of reducing equivalents per laser flash, which may result from the loss of the primary donor (semicarbazide) by formation of the semicarbazone with pyruvate. This would not be expected to alter the kinetics of protein reduction, since pseudo-first-order conditions were ensured by providing an excess of protein acceptor, and this expectation was supported by control experiments.

Occasionally, addition of stock solutions of sodium pyruvate resulted in mixed kinetic behavior, suggesting the presence of both liganded and unliganded protein. The degree of mixed kinetic behavior increased upon long-term storage of the solid sodium pyruvate at 5 °C, and was observed to vary with the lot number of the solid sodium pyruvate from the supplier. This kinetic behavior was interpreted as a result of the presence

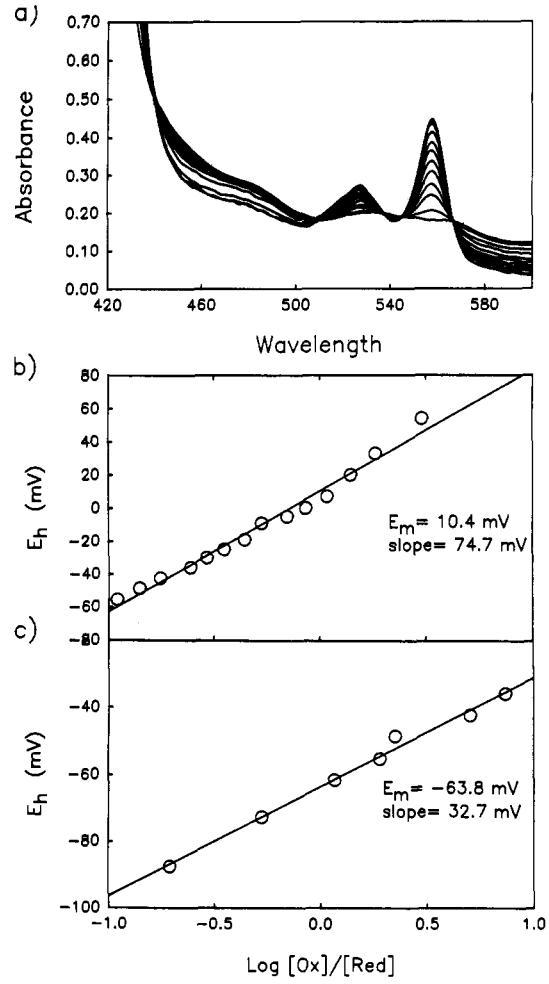

FIGURE 5: (a) Absorption spectra obtained during potentiometric titration of flavocytochrome in the absence of pyruvate. Buffer conditions were 5.7 mM phosphate, pH 7.0, containing 0.5 mM EDTA and 87 mM NaCl; I = 100 mM. Nernst plots constructed from the absorbance changes corresponding to the reduction of (b) heme and (c) FMN cofactors.

of an impurity formed upon decomposition of the sodium pyruvate. Presumably, this impurity binds to the protein competitively with pyruvate, leading to mixed kinetic behavior. Consistent with this interpretation, recrystallization of sodium pyruvate from a water/ethanol solution, followed by storage under P_2O_5 at −15 °C, removed all indication of mixed kinetic behavior.

Potentiometric Titration of Flavocytochrome b_2. Previous studies performed with the flavocytochrome b_2 from *Hansenula anomala* (Tegoni et al., 1984, 1986) have demonstrated that the semiquinone form of the FMN cofactor is significantly stabilized in the presence of pyruvate. This results from an increase in the midpoint potential of the F_{ox}/F_{sq} redox couple and a decrease in the midpoint potential of the F_{sq}/F_{red} couple, relative to the values obtained in the absence of pyruvate. Such changes alter the driving force for intramolecular electron transfer between the FMN semiquinone and heme cofactor, and could be a factor in controlling the rate of this process. Thus, it was of interest to determine the midpoint potentials of the FMN and heme cofactors of flavocytochrome b_2 from *Saccharomyces* in the absence and presence of pyruvate.

Difference spectra obtained during the potentiometric titrations of the flavocytochrome in the absence of pyruvate are presented in Figure 5a. The majority of the absorbance increase at 557 nm was observed to precede the absorbance bleach at 450 nm. Since spectral changes at the former

wavelength are dominated by the reduction of heme, while those at the latter wavelength contain equal contributions from heme and flavin reduction, this implies that the midpoint potentials of the heme and FMN cofactors are well separated under these conditions. Nernst plots constructed by using absorbance changes at 557 nm yielded a midpoint potential of +10 mV for the H_{ox}/H_{red} couple (n = 0.85 e^-; Figure 5b). This value is consistent with that reported in the literature for the heme potential of the cleaved form of flavocytochrome b_2 from *Saccharomyces* (Capeillere-Blandin et al., 1975). Nernst plots constructed from the absorbance changes at 450 nm, following the removal of contributions from heme reduction, gave a two-electron midpoint potential for the FMN cofactor (F_{ox}/F_{red}) of −64 mV (n = 1.9 e^-; Figure 5c). This value is, again, comparable to that obtained previously from EPR measurements using the cleaved form of the flavocytochrome from *Saccharomyces* (Capeillere-Blandin et al., 1975). Estimates for the first and second one-electron reduction potential of the FMN cofactor (E_1, and E_2, respectively) can be obtained from the deviation in the Nernst slope from that of the theoretical slope for a two-electron redox process (Clark, 1960). The observed value of 1.9 indicates significant destabilization of the FMN semiquinone, relative to the fully reduced FMN. Inasmuch as a different of −60 mV or more between E_1 and E_2 would result in the accumulation of less than 10% semiquinone during the titration (as observed), the results suggest estimates of −94 and −34 mV for the F_{ox}/F_{sq} redox couple (E_1) and for the F_{sq}/F_{red} couple (E_2), respectively. Thus, we can conclude that there is a *minimum* value of +100 mV for the thermodynamic driving force for electron transfer from FMN semiquinone to b_2 heme. This difference is greater than that reported previously (+60 mV; Capeillere-Blandin et al., 1975) and may result from the use of the cleaved form of flavocytochrome b_2 in the earlier study.

In the presence of pyruvate, difference spectra collected during the titration of flavocytochrome indicate that the absorbance changes at 557 nm occur concurrently with those at 450 nm (Figure 6a), in contrast to what was observed in the absence of pyruvate. Nernst plots constructed from the absorbance changes at 557 nm yielded a midpoint potential of +8.5 mV for the H_{ox}/H_{red} couple (n = 0.9 e^-; Figure 6b). This value is essentially unchanged from that obtained in the absence of pyruvate, consistent with previous reports using the protein isolated from *Hansenula* (Tegoni et al., 1984, 1986). Nernst plots constructed from the absorbance changes at 450 nm gave a midpoint potential of +3.8 mV for the FMN cofactor (n = 1.1 e^-; Figure 6c). The slope of the Nernst plot in Figure 6c clearly indicates a one-electron process, which is interpreted as that of the F_{ox}/F_{sq} redox couple (E_1). Thus, the inclusion of pyruvate during the titration resulted in a more positive value for the observed midpoint potential, which must be a consequence of an increase in E_1. This is consistent with the previous results using the protein isolated from *Hansenula* (Tegoni et al., 1984, 1986).

It was not possible from the present experiments to determine the midpoint potential of the F_{sq}/F_{red} couple (E_2) in the presence of pyruvate, since an appropriate wavelength was not available to monitor the loss of FMN semiquinone or the formation of the FMN hydroquinone. However, the results suggest that the midpoint potential of the F_{sq}/F_{red} couple must be at least 60 mV more negative than the F_{ox}/F_{sq} couple, i.e., $E_2 < -55$ mV. For comparison, the reported E_2 for the FMN of *Hansenula* flavocytochrome b_2 is −133 mV in the presence of pyruvate (as determined by EPR), which is 70 mV more negative than the corresponding value obtained in the absence

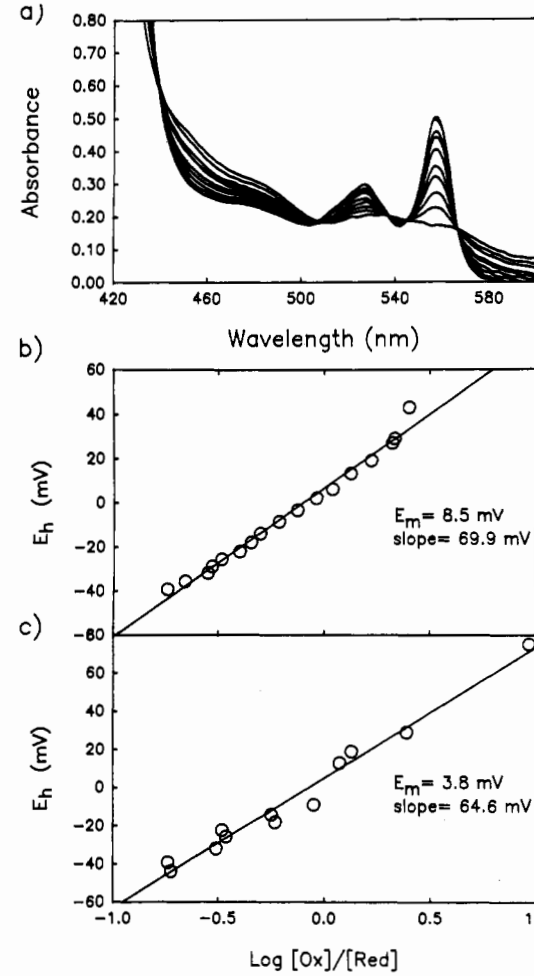

FIGURE 6: (a) Absorption spectra obtained during potentiometric titration of flavocytochrome in the presence of pyruvate. Buffer conditions were 5.7 mM phosphate, pH 7.0, containing 0.5 mM EDTA, 87 mM NaCl, and 5 mM sodium pyruvate; I = 100 mM. Nernst plots constructed from the absorbance changes corresponding to the reduction of (b) heme and (c) FMN cofactors.

of pyruvate (Tegoni et al., 1986).

The midpoint potentials of the heme and FMN cofactors of the *Saccharomyces* flavocytochrome, obtained in the presence of pyruvate, were unaffected by changes in ionic strength (not shown). Therefore, the ionic strength dependent changes observed in the rate constant for intramolecular electron transfer (see above) were not a result of changes in midpoint potential.

The observed rate constants reported for the intramolecular electron transfer in the presence of pyruvate represent the sum of the forward and reverse microscopic rate constants for electron transfer between FMN semiquinone and oxidized heme, i.e.:

$$F_{sq}\text{–}H_{ox} \underset{k_r}{\overset{k_f}{\rightleftharpoons}} F_{ox}\text{–}H_{red}$$

Values for k_f and k_r can be calculated from the equilibrium constant for the reaction ($K_{eq} = k_f/k_r$), which is in turn obtained from the midpoint potential difference between the one-electron redox couples of FMN (i.e., E_1) and heme. A potential difference of approximately +5 mV was determined for the *Saccharomyces* protein in the presence of pyruvate (see above), which indicates a K_{eq} of 1.22. Values for k_f and k_r calculated from the observed rate constants are presented in Table I. Values for enzymatic turnover (expressed in terms of moles of substrate oxidized per mole of monomeric heme) are included for comparison. In all cases, the calculated

Table I: Microscopic Rate Constants[a] for Electron Transfer between FMN Semiquinone and Oxidized Heme Cofactors of Flavocytochrome b_2, in the Presence of Pyruvate

[phosphate] (mM)	I (mM)	k_{obs} (s^{-1})	k_f (s^{-1})	k_r (s^{-1})	TN[b] (s^{-1})
5.7	10	1200	660	540	180
5.7	100	770	420	350	220
5.7	505	400	220	180	190
50	95	610	335	275	230
100	185	520	285	235	230

[a] Forward and reverse rate constants correspond to the equation presented in the text and were calculated from the observed rate constants and equilibrium constants as described in the text. [b] Steady-state turnover numbers are expressed in terms of moles of substrate oxidized per mole of monomeric heme at 25 °C.

forward rate constant is consistent with enzymatic turnover.

Discussion

The present kinetic experiments demonstrate that intramolecular electron transfer between the FMN and heme cofactors of the flavocytochrome b_2 from *Saccharomyces* was observed only in the presence of pyruvate. This is surprising in that the driving force for electron transfer from FMN semiquinone to oxidized heme is much greater in the absence of pyruvate (+100 mV vs approximately +5 mV for the *Saccharomyces* protein; see above) and the geometry of the cofactors (Xia & Mathews, 1990) appears to be favorable for intramolecular electron transfer. The *simplest* explanation for this behavior is that electron transfer between the cofactors is inhibited (for reasons presently unknown) in the unliganded enzyme and that the binding of pyruvate induces a conformation change which permits electron transfer to occur. The present experiments do not exclude the possibility that substrate (i.e., L-lactate) binding also induces a similar conformational change which facilitates communication between the flavin and the heme sites. In this context, however, it should be noted that Tegoni et al. (1990), on the basis of simulations of steady-state kinetic data for the *Hansenula* flavocytochrome b_2, have concluded that the binding of pyruvate *decreases* the rate constants for electron transfer from the flavin semiquinone both to the b_2 heme (intramolecularly) and to ferricyanide (intermolecularly) [cf. also Tegoni et al. (1984a,b, 1986)]. More work is required in order to determine the basis for this apparent discrepancy in the interpretation of the effects of pyruvate on flavocytochrome b_2.

The X-ray crystal structure of flavocytochrome b_2 (Xia & Mathews, 1990) has demonstrated that the presence of pyruvate at the substrate binding site is associated with a disordered cytochrome domain, which implies a greater mobility of this region of the protein. In contrast, the cytochrome domain is clearly resolved in those subunits which do not contain pyruvate at the active site. More subtle differences in protein conformation were observed within the flavodehydrogenase domain of those subunits which contained pyruvate. Tyrosine-143 is an example of one such residue within the latter domain that is influenced by the presence of pyruvate. The aromatic ring of this amino acid lies between the FMN and heme, and is approximately perpendicular to the plane of these cofactors. Furthermore, this residue is hydrogen-bonded to the propionate of the heme A ring in those subunits which do not contain pyruvate. Increased mobility of the cytochrome domain and/or motion of Tyr-143 within the flavodehydrogenase domain could be associated with the different kinetic results observed in the presence and absence of pyruvate. Such structural changes could provide the basis for a conformational gating mechanism (Hoffman & Ratner, 1987), which may be involved in the regulation of electron transfer in multi-redox-center proteins (Brzezinski & Malmström, 1987) or within protein–protein complexes (Hazzard et al., 1988; Peerey et al., 1990). This requires further study.

The ionic strength dependent behavior displayed by the rate constant for intramolecular electron transfer from FMN semiquinone to b_2 heme may also have a structural basis. The flavodehydrogenase and cytochrome domains are well distinguished in the crystal structure of the pyruvate-free subunit. The interface regions of the two domains display appreciable structural complementarity (Xia & Mathews, 1990). However, the only charge pair in this interface region is that between the propionate of the heme D ring and Lys-296 of the flavodehydrogenase domain. This interaction could serve to help orient the heme cofactor relative to the reduced FMN prior to electron transfer, and thus may be responsible for the observed ionic strength effects. This also requires further investigation.

Potentiometric titrations performed with *Saccharomyces* flavocytochrome b_2 in the absence and presence of pyruvate demonstrate that profound changes in the redox behavior of the FMN cofactor occur as a result of pyruvate binding. Qualitatively similar results have been observed by using the protein from *Hansenula* (Tegoni et al., 1984, 1986). Although these changes in midpoint potentials for the E_1 and E_2 couples of the FMN cofactor may facilitate the coupling of a two-electron oxidation reaction with a one-electron transfer process, they cannot account for the kinetic differences observed in the absence and presence of pyruvate.

Electron transfer between redox cofactors of flavocytochrome b_2 subsequent to substrate reduction has been examined previously by rapid-mixing techniques (Ogura & Nakamura, 1966; Suzuki & Ogura, 1970; Capeillere-Blandin, 1975; Capeillere-Blandin et al., 1975, 1986; Pompon et al., 1980). Although direct measurements of intramolecular electron transfer could not be made in these experiments due to the rate limitation imposed by the reduction of the FMN cofactor by substrate, rate constants for the intramolecular process have been estimated by computer simulations (Capeillere-Blandin, 1975; Pompon, 1980; Capeillere-Blandin et al., 1986). Early simulations suggested estimates of 600 and 100 s^{-1} for the forward and reverse rate constants for electron transfer within the flavocytochrome from *Saccharomyces* (Capeillere-Blandin, 1975) in 0.1 M phosphate buffer, pH 7.36, at 24 °C. Additional values have been reported for both the *Hansenula* and *Saccharomyces* flavocytochromes from simulations of rapid-mixing experiments performed at lower temperatures (5 °C; Pompon, 1980; Capeillere-Blandin et al., 1986). These estimates are significantly larger than the values reported here. However, it must be kept in mind that the rate constants for k_f and k_r obtained from simulations of stopped-flow traces correspond to one-electron transfer from $FMNH_2$ to H_{ox} (the first catalytically relevant intramolecular electron-transfer process), while the values reported here represent electron transfer from FMN_{sq} to H_{ox}, which is the second intramolecular step in catalysis. On the basis of Marcus theory (Marcus & Sutin, 1985), it is not unreasonable to expect that the rate constant for electron transfer from $FMNH_2$ to H_{ox} would be larger than that for FMN_{sq} to H_{ox} because of the greater driving force.

More recently, Janot et al. (1990) have observed a biphasic time course for the reoxidation of *Hansenula* flavocytochrome b_2 by cytochrome *c*. Again on the basis of kinetic simulations, they assigned the slow phase (k = 5 s^{-1} at 5 °C) to the intramolecular electron-transfer step from the pyruvate-liganded

flavin semiquinone to the b_2 heme, although the intramolecular nature of this transient was not established experimentally. These workers also concluded that pyruvate acts to slow down the rate of intramolecular electron transfer, based on a comparison of their results with the earlier studies of Tegoni et al. (1984b) (see above).

In the present experiments, the effects of pyruvate on both the kinetic behavior and the potentiometric titrations were found to be essentially complete at a concentration of 5 mM. This does not appear consistent with a K_i of 3.7 mM for inhibition of the steady-state oxidation of L-lactate by pyruvate (using ferricyanide as the final acceptor; see above), and thus would suggest that the affinity of the flavocytochrome for pyruvate is stronger than the K_i value indicates. Although we have not directly determined this affinity, it should be noted that the inhibition of the enzyme by pyruvate is complex and that significant differences have been noted previously between the steady-state turnover of the enzyme when ferricyanide was used as the final acceptor in place of cytochrome *c* [cf. Tegoni et al. (1990)].

Comparisons of the time-resolved and steady-state difference spectra suggested that 30–40% of the reducing equivalents generated during the laser flash resulted in reduction of the FMN cofactor in the absence of pyruvate. However, the reduction of heme due to intermolecular electron transfer from FMN semiquinone only corresponded to 20–25% of the total signal observed at 557 nm. The redox potential measurements suggest that *complete* reoxidation of FMN_{sq} should have occurred. Although this is only a small discrepancy, it is significantly larger than can be accounted for by experimental error. If disproportionation of the FMN semiquinone proceeded on the same time scale as the intermolecular electron transfer, this could account for the difference. However, due to the nature of the isosbestic point at 438.5 nm, and the optical system used, it was not possible to detect the formation of $FMNH_2$ during flash photolysis experiments. Another possibility is that the flavin–heme interactions within the flavocytochrome modulate the redox potentials for one-electron and two-electron reduced forms, resulting in a difference between the transient and equilibrium situations. This requires further study.

A similar discrepancy was observed for the slow intramolecular electron transfer in the presence of pyruvate. Although the direction of the transfer is consistent with the redox potential measurements, the reoxidation of heme by intramolecular electron transfer to FMN in the presence of pyruvate only corresponded to 20–30% of the total signal observed at 557 nm. Such an equilibrium distribution is not consistent with an observed midpoint potential difference of only 5–10 mV. Although a definitive explanation for this discrepancy is not presently available, this may be a further indication of cooperativity between the H_{ox}/H_{red} and F_{ox}/F_{red} redox couples during the potentiometric titration of flavocytochrome.

Registry No. dLfS, 133495-48-4; FMN semiquinone, 34469-63-1; pyruvic acid, 127-17-3; flavocytochrome b_2, 9078-32-4; heme, 14875-96-8.

References

Baudras, A. (1962) *Biochem. Biophys. Res. Commun. 7*, 310–314.

Baudras, A. (1965) *Bull. Soc. Chim. Biol. 47*, 1143–1175.

Bhattacharyya, A. K., Tollin, G., Davis, M., & Edmondson, D. E. (1983) *Biochemistry 22*, 5270–5279.

Blankenhorn, G. (1976) *Eur. J. Biochem. 67*, 67–80.

Blazy, B. (1982) Thèse de Doctorat d'Etat, University of Toulouse.

Brzezinski, P., & Malmström, B. G. (1987) *Biochim. Biophys. Acta 894*, 29–38.

Capeillere-Blandin, C. (1975) *Eur. J. Biochem. 56*, 91–101.

Capeillere-Blandin, C. (1982) *Eur. J. Biochem. 128*, 533–542.

Capeillere-Blandin, C., & Albani, J. (1987) *Biochem. J. 245*, 159–165.

Capeillere-Blandin, C., Bray, R. C., Iwatsubo, M., & Labeyrie, F. (1975) *Eur. J. Biochem. 54*, 549–566.

Capeillere-Blandin, C., Iwatsubo, M., Testylier, G., & Labeyrie, F. (1980) *Flavins Flavoproteins, Proc. Int. Symp., 6th*, 617–630.

Capeillere-Blandin, C., Pucheault, J., & Ferradini, C. (1984) *Biochim. Biophys. Acta 786*, 67–78.

Capeillere-Blandin, C., Barber, M. J., & Bray, R. C. (1986) *Biochem. J. 238*, 745–756.

Clark, W. M. (1960) *Oxidation–Reduction Potentials of Organic Systems*, The Williams and Wilkins Co., Baltimore, MD.

Cleland, W. W. (1963) *Biochim. Biophys. Acta 67*, 173–187.

Ferguson-Miller, S., Brautigan, D. L., & Margoliash, E. (1976) *J. Biol. Chem. 251*, 1104–1115.

Gopal, D., Wilson, G. S., Earl, R. A., & Cusanovich, M. A. (1988) *J. Biol. Chem. 263*, 11652–11656.

Hazzard, J. T., McLendon, G., Cusanovich, M. A., Das, G., Sherman, F., & Tollin, G. (1988) *Biochemistry 27*, 4445–4451.

Heelis, P. F., Parsons, B. J., Phillips, G. O., & Swallow, A. J. (1989) *Int. J. Radiat. Biol. 55*, 557–562.

Hoffman, B. M., & Ratner, M. A. (1987) *J. Am. Chem. Soc. 109*, 6237–6243.

Jacq, C., & Lederer, F. (1974) *Eur. J. Biochem. 41*, 311–320.

Janot, J. M., Capeilleire-Blandin, C., & Labeyrie, F. (1990) *Biochim. Biophys. Acta 1016*, 165–176.

Labeyrie, F. (1982) *Flavins Flavoproteins, Proc. Int. Symp., 7th*, 823–832.

Labeyrie, F., Groudinsky, O., Jacquot-Armand, Y., & Naslin, L. (1966) *Biochim. Biophys. Acta 128*, 492–503.

Labeyrie, F., Baudras, A., & Lederer, F. (1978) *Methods Enzymol. 53*, 238–256.

Lederer, F. (1974) *Eur. J. Biochem. 46*, 393–399.

Lederer, F. (1978) *Eur. J. Biochem. 88*, 425–431.

Malatesta, F., Antonini, G., Sarti, P., & Brunori, M. (1987) *Biochem. J. 248*, 161–165.

Marcus, R. A., & Sutin, N. (1985) *Biochim. Biophys. Acta 811*, 256–322.

Mathews, F. S., & Xia, Z.-X. (1987) *Flavins Flavoproteins, Proc. Int. Symp., 9th*, 123–132.

Matsushima, A., Yoshimura, T., & Aki, K. (1986) *J. Biochem. 100*, 543–551.

Ogura, Y., & Nakamura, T. (1966) *J. Biochem. 60*, 77–86.

O'Reilly, J. E. (1973) *Biochim. Biophys. Acta 292*, 509–515.

Peerey, L. M., Hazzard, J. T., Tollin, G., & Kostic, N. M. (1991) *Biochemistry* (submitted for publication).

Pompon, D. (1980) *Eur. J. Biochem. 106*, 151–159.

Pompon, D., Iwatsubo, M., & Lederer, F. (1980) *Eur. J. Biochem. 104*, 479–488.

Przysiecki, C. T., Bhattacharyya, A. K., Tollin, G., & Cusanovich, M. A. (1985) *J. Biol. Chem. 260*, 1452–1458.

Reid, G. A., White, S., Black, M. T., Lederer, F., Mathews, F. S., & Champman, S. K. (1988) *Eur. J. Biochem. 178*, 329–333.

Smit, P., Stork, G. A., van der Plas, H. C., den Hartog, J. A. J., van der Marel, G. A., & van Boom, J. H. (1986) *Recl. Trav. Chim. Pays-Bas 105*, 538–544.

Stankovich, M. T. (1980) *Anal. Biochem. 109*, 295-308.
Suzuki, H., & Ogura, Y. (1970) *J. Biochem. 67*, 277-289.
Tegoni, M., Janot, M. C., Silvestrini, M., Brunori, M., & Labeyrie, F. (1984a) *Biochem. Biophys. Res. Commun. 118*, 753-759.
Tegoni, M., Silvestrini, M. C., Labeyrie, F., & Brunori, M. (1984b) *Eur. J. Biochem. 140*, 39-45.
Tegoni, M., Janot, J. M., & Labeyrie, F. (1986) *Eur. J. Biochem. 155*, 491-503.
Tegoni, M., Janot, J. M., & Labeyrie, F. (1990) *Eur. J. Biochem. 190*, 329-342.
Visser, A. J. W. G., & Fendler, J. H. (1982) *J. Phys. Chem. 86*, 2406-2409.
Wilson, G. S. (1978) *Methods Enzymol. 54*, 396-410.
Xia, Z., & Mathews, F. S. (1990) *J. Mol. Biol. 212*, 837-863.
Xia, Z.-X., Shamala, N., Bethge, P. H., Lim, L. W., Bellamy, H. D., Xuong, N. H., Lederer, F., & Mathews, F. S. (1987) *Proc. Natl. Acad. Sci. U.S.A. 84*, 2629-2633.

Shape and Lipid-Binding Site of the Nonspecific Lipid-Transfer Protein (Sterol Carrier Protein 2): A Steady-State and Time-Resolved Fluorescence Study

Theodorus W. J. Gadella, Jr.,*,‡ Philippe I. H. Bastiaens,§ Antonie J. W. G. Visser,§ and Karel W. A. Wirtz‡
Center for Biomembranes and Lipid Enzymology, State University of Utrecht, Padualaan 8, 3584 CH Utrecht, The Netherlands, and Department of Biochemistry, Agricultural University, Dreijenlaan 3, 6703 HA Wageningen, The Netherlands
Received November 5, 1990; Revised Manuscript Received February 12, 1991

ABSTRACT: The nonspecific lipid-transfer protein (nsL-TP) from bovine liver was studied with time-resolved and steady-state fluorescence techniques. From the decay of the intrinsic tryptophanyl fluorescence, it was estimated that the rotational correlation time of nsL-TP is 15 ns. This parameter increased only slightly upon addition of an excess of negatively charged vesicles, indicating that the basic nsL-TP is not immobilized at the membrane surface under these conditions. Binding studies using fluorescent lipid analogues revealed that nsL-TP is able to extract *sn*-2-(pyrenehexanoyl)phosphatidylcholine and 1-palmitoyl-2-[3-(diphenylhexatrienyl)propionyl]-*sn*-3-phosphocholine (DPHp-PC) from a quenched donor vesicle. The fluorescence increase resulting from this binding was poorly quenched by either acrylamide or iodide. This indicates that nsL-TP shields the bound PC molecules from the aqueous environment. Time-resolved analysis of DPH fluorescence originating from DPHp-PC bound to nsL-TP yielded a rotational correlation time of 7.4 ns. This correlation time strongly suggests that the DPH moiety of the bound molecule is immobilized and that the nsL-TP/DPHp-PC complex is not attached to the donor vesicle. In view of the longer rotational correlation time obtained for the intrinsic tryptophanyl fluorescence, we conclude that nsL-TP is highly asymmetric. The data are consistent with a model in which the shape of nsL-TP is ellipsoidal with an axis ratio of 2.8. The implications for the mode of action of nsL-TP are discussed.

The nonspecific lipid-transfer protein (nsL-TP),[1] also called sterol carrier protein 2, is one of the intracellular hydrophobic ligand binding/transfer proteins (Scallen et al., 1985; Helmkamp, 1986; Wirtz & Gadella, 1990). The protein has been purified from rat, bovine, goat, and human liver (Bloj & Zilversmit, 1977; Crain & Zilversmit, 1980; Noland et al., 1980; Poorthuis & Wirtz, 1983; Traszkos & Gaylor, 1983; Van Amerongen et al., 1987; Basu et al., 1988). The high sequence homology between rat and bovine nsL-TP (>90%) suggests an important role for the protein in cellular processes (Westerman & Wirtz, 1985; Pastuszyn et al., 1987; Morris et al., 1988). NsL-TP stimulates, in vitro, the intermembrane transfer of various lipid classes including cholesterol (Crain & Zilversmit, 1980; Chanderbhan et al., 1982; Muczynski & Stahl, 1983; North & Fleischer, 1983; Van Amerongen et al., 1989), phospholipids (Crain & Zilversmit, 1980; Nichols, 1988; Van Amerongen et al., 1989), sphingomyelin (Crain & Zilversmit, 1980), gangliosides (Bloj & Zilversmit, 1981), and neutral glycosphingolipids (Bloj & Zilversmit, 1981). As a consequence of nsL-TP-mediated transfer of cholesterol, nsL-TP was shown to stimulate microsomal conversion of lanosterol into cholesterol (Noland et al., 1980; Traszkos & Gaylor, 1983), cholesterol esterification (Gavey et al., 1981; Poorthuis & Wirtz, 1982; Traszkos & Gaylor, 1983), bile acid formation (Seltman et al., 1985; Lidström-Olssen & Wikvall, 1986), and steroid hormone synthesis (Chanderbhan et al., 1982; Vahouny et al., 1983; Van Noort et al., 1986, 1988a,b). Although many studies have focused on the role of nsL-TP in lipid metabolism, the exact mechanism by which nsL-TP mediates the transfer of cholesterol and of phospholipids is not yet fully understood. Recently it was shown that upon equilibration with membranes containing dehydroergosterol, nsL-TP forms a water-soluble lipid/nsL-TP complex (Schroeder et al., 1990). This strongly suggests that the lip-

‡Center for Biomembranes and Lipid Enzymology, State University of Utrecht.
§Department of Biochemistry, Agricultural University.

[1] Abbreviations: nsL-TP, nonspecific lipid-transfer protein; PC, phosphatidylcholine; TNP-PE, *N*-(2,4,6-trinitrophenyl)phosphatidylethanolamine; PA, phosphatidic acid; Pyr(6)-PC, *sn*-2-(pyrenehexanoyl)phosphatidylcholine; DPH, 1,6-diphenyl-1,3,5-hexatriene (all trans); DPHp-PC, 1-palmitoyl-2-[3-(diphenylhexatrienyl)propionyl]-*sn*-3-phosphocholine; TLC, thin-layer chromatography; SDS-PAGE, sodium dodecyl sulfate-polyacrylamide gel electrophoresis; POPOP, 1,4-di-[2-(5-phenyloxazolyl)]benzene; PTF, *p*-terphenyl; IgG, immunoglobulin G; PI-TP, phosphatidylinositol-transfer protein; PC-TP, phosphatidylcholine-transfer protein; BSA, bovine serum albumin; Tris, tris(hydroxymethyl)aminomethane; EDTA, ethylenediaminetetraacetic acid; EGTA, ethylene glycol-bis-(β-aminomethyl ether)-*N*,*N*,*N*′,*N*′-tetraacetic acid; DMSO, dimethyl sulfoxide; DW, Durbin-Watson parameter.

0006-2960/91/0430-5555$02.50/0